Closed-loop Neuronal Computations: Focus on Vibrissa Somatosensation in Rat

Ehud Ahissar[1,4] and David Kleinfeld[2–4]

[1]Department of Neurobiology, The Weizmann Institute of Science, Rehovot 76100, Israel, [2]Department of Physics and [3]Graduate Program in Neurosciences, University of California at San Diego, La Jolla, CA 92093 and [4] Institute for Theoretical Physics, University of California at Santa Barbara, Santa Barbara, CA 93106, USA

Two classes of neuronal architectures dominate in the ongoing debate on the nature of computing by nervous systems. The first is a predominantly feedforward architecture, in which local interactions among neurons within each processing stage play a less influential role compared with the drive of the input to that stage. The second class is a recurrent network architecture, in which the local interactions among neighboring neurons dominate the dynamics of neuronal activity so that the input acts only to bias or seed the state of the network. The study of sensorimotor networks, however, serves to highlight a third class of architectures, which is neither feedforward nor locally recurrent and where computations depend on large-scale feedback loops. Findings that have emerged from our laboratories and those of our colleagues suggest that the vibrissa sensorimotor system is involved in such closed-loop computations. In particular, single unit responses from vibrissa sensory and motor areas show generic signatures of phase-sensitive detection and control at the level of thalamocortical and corticocortical loops. These loops are likely to be components within a greater closed-loop vibrissa sensorimotor system, which optimizes sensory processing.

Introduction

Information flows into the brain in a feedforward manner from the sensory neurons up through brainstem and thalamic nuclei and into the cortex. This feedforward organization allows successive transformations of information and generation of internal representations (Rumelhart and McClelland, 1986). However, the brain also contains an enormous amount of recurrent and feedback connections at various levels. The possible function of recurrent connections, i.e. connections between neurons at the same level of processing, has been intensively investigated. One of the more attractive suggestions for such a function has come from analogies with the statistical mechanics of many particle systems: recurrent networks could function as associative networks for memory (Hopfield, 1982; Amit, 1989), as well as continuous attractors for sensory coding (Ben-Yishai *et al*., 1995) or motor control (Seung, 1996). These networks, in their most basic form, are largely homogeneous so that all neurons participating in such a network have a similar role in computation.

Feedforward and recurrent computation schemes can be reconciled by viewing information as being passed from one processing station to another in a feedforward manner and processed at each station by recurrent networks (Fig. 1*a*). However, the description of brain architecture is not complete without inclusion of its third major component – large-scale feedback connections. Feedback connections, which feed the output of the receiving areas back to the transmitting areas, occur at all levels (Fig. 1*b*). Cortico-thalamic feedback connections are perhaps the most intensively studied example of this kind. Feedback connections, however, occur not only between cortex and thalamic nuclei, but also between cortex and brainstem, between cortical areas that are connected via feedforward connections, and from motor output nuclei back to the cortex; see Kleinfeld *et al*. (Kleinfeld *et al*., 1999) for a review on the vibrissa sensorimotor system.

About 50 years ago, the pioneering control theorist Norbert Wiener suggested that some basic operations of the nervous system are based on servo loops (Wiener, 1949). Servo loops are systems whose aim is to keep an output variable within a predetermined range. These loops use feedback to determine the actual state of the output variable and a comparator circuit to compare this value with the target value. For example, keeping a stick upright using one finger requires a servo operation. A servo loop is a particular type of closed-loop system. In general, closed-loop systems can be used to accomplish various decoding, transformation and control tasks. Such tasks are routinely performed in the brain.

The architecture of closed-loop systems lies between that of feedforward and recurrent networks. Like in feedforward networks, but unlike in recurrent networks, the flow of information in closed-loop systems is well delineated. Like in recurrent networks, but unlike in feedforward networks, information flows in both directions, i.e. from input to output and back. Thus, closed-loop circuits provide a substrate for computations that cannot be done with purely feedforward or recurrent configurations. One example is iterative transformations from one set of neuronal variables to another, as may occur in the encoding and processing of sensory inputs.

Closed-loop dynamics can be found at all levels of neuronal function. At the molecular level, the activity of a biochemical process can be suppressed (negative feedback) or enhanced (positive feedback) by the end product of that process. Similarly, at the cellular level, the opening of ion channels is a function of the membrane potential, which in turn is affected by ion channel opening. At the circuit level, the activity of individual neurons influences neighboring cells, whose activity in turn modulates that of the original cell. At the system level, e.g. the level of cortical areas and sub-cortical nuclei, each neuronal circuit affects several other circuits whose output ultimately feeds back on the original circuit. At the behavioral level, sensory input guides the motor response, which in turn updates the input to the sensory system. We focus here on the circuit, system and behavioral levels.

Computations Performed by Neuronal Closed Loops

The operation of neuronal closed loops at various levels can be considered from either homeostatic or computational points of view. All closed loops have set-points at whiche the values of their state variables are stable. Thus, feedback loops provide a mechanism for maintaining neuronal variables within a particular range of values. This can be termed a homeostatic function. On the other hand, since the feedback loops compute changes in the state variables to counteract changes in the

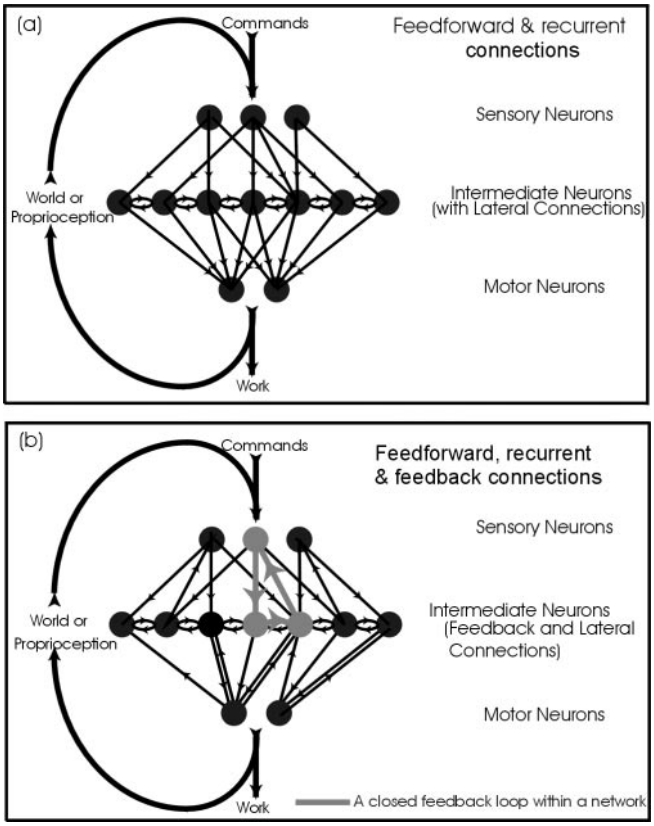

Figure 1. Diagram of generalized neuronal architectures. (*a*) An architecture that is a mixture of feedforward and recurrent connections. The flow of information between populations of neurons is largely feedforward and, within populations, largely recurrent. The system as a whole is closed only through the outside world, e.g. sensations brought about by changes in the position of an actuator (e.g. a limb). Thus, feedback is predominantly through the direct sensation of motor output, through proprioception, or through the effect of the motor movement on the outside world. (*b*) An architecture that is a mixture of feedforward, recurrent and feedback connections. The flow of information is both feedforward and feedback along closed loops. Neuronal closed loops are illustrated by the gray-colored neuronal elements. In this case there is substantial feedback, both through intrinsic neuronal connections and through the outside world.

external world, the change in state variables constitutes a representation of change in the outside world. As an example, we consider Wiener's description of the sensorimotor control of a stick with one finger. The state variables are the angle of the stick and the position (angle and pivot location) of the finger. When the stick leaves a set-point as a result of a change in local air pressure, the sensorimotor system will converge to a new set-point in which the position of the finger is different. The end result, from the homeostatic point of view, is that equilibrium is re-established. From the computational point of view, the new set-point is an internal representation of the new conditions, e.g. the new local air pressure, in the external world. (We note that the representation of perturbation by state variables may be dimensionally under- or over-determined and possibly not unique.) This internal representation is 'computed' by the closed-loop mechanism.

Closed loops provide an elegant solution to control problems that involve different types of variables, such as the control of mechanical variables by neuronal variables. To illustrate closed-loop control, we will consider two schemes that are implemented by a 'low-level' loop, the stretch-reflex loop, under 'high-level' descending control.

Examples of Motor Control by Closed Loops

A skeletal joint consists of muscles, arranged as pairs with opposing directions of torque, that quasistatically maintain the joint at a desired angle under the presence of a load (Fig. 2*a*). The pairs of muscles are arranged as synergists, i.e. muscles that close the joint, and antagonists, i.e. muscles that open the joint. There are two forms of feedback sensors at a joint. The first are spindles, which encode the degree of muscle-stretch. To the extent that the angle is proportional to the stretch, the spindles are reporters of the angle of the joint. The second are Golgi tendons, which report the force produced by the muscle or, equivalently, the torque. Both of these receptors form a large-scale feedback path from the joint back to the motor neurons (Fig. 2*b*,*c*). For simplicity, we will consider only positional feedback.

A first feedback scheme considers the control of the absolute angle of a joint. This control scheme makes use of a descending command (θ_0 in Fig. 2*b*), generated by higher neuronal circuits. The absolute position of the joint (θ in Fig. 2*b*), as encoded by the spindles, is compared with the command (Δ operation in Fig. 2*b*) and used to generate a control signal of the form $d\theta/dt = G(\theta-\theta_0)$. This signal, in turn, drives the synergistic motor neurons and its negated form (mediated by inhibitory interneurons) drives antagonist motor neurons. Under steady-state conditions, the two muscle groups integrate the control signal. For a sufficiently large gain (G in Fig. 2*b*), the angle of the joint will converge on the desired angle, i.e. $\theta \approx \theta_0$.

A second feedback scheme, which is of relevance to our discussion on the vibrissa sensorimotor system, considers the periodic modulation of the angle of a joint. This control scheme makes use of a descending signal that oscillates in time ($\cos 2\pi f_0 t$ in Fig. 2*c*). The position of the joint ($\cos[2\pi f_0 t + \phi]$ in Fig. 2c) is mixed with the control signal, as could occur by neurons or small networks of neurons that use their threshold properties to multiply their inputs [X in Fig. 2*b*; see Ahissar (Ahissar, 1998) and Ahrens *et al.* (Ahrens *et al.*, 2002)]. The spectrum of the mixed signal contains the difference between the desired frequency and the actual frequency ($f - f_0$), as well as the sum of these frequencies. The low (difference) frequencies are extracted from the mixed signal by the low-pass filtering properties of the involved neurons. The final signal contains a constant ($G\sin\phi$ in Fig. 2*c*), as well as a term, which for small frequency differences (i.e. $f \approx f_0$) is proportional to the phase slippage [$O\{(f - f_0)t\}$ in Fig. 2*c*]. This final signal is used to drive a local oscillator in the spinal cord (~ in Fig. 2c), for which the oscillation frequency is a monotonic function of the input. For open-loop gains (i.e. accumulated gain along the loop) around 1, the frequency of the local oscillator will be driven to match that of the control signal, so that under steady-state conditions $f = f_0$ and the final signal is a constant with no phase slippage. Thus there is a constant phase difference, ϕ, between the reference and spinal oscillators, which is a monotonic function of $(f - f_0)/G$. By combining feedback schemes for both position and oscillation control, a joint can oscillate around a desired position, as is required for certain motor tasks, such as walking.

Transformations from one variable to another are required not only for motor control, but also for sensory processing. Perceived entities are composed of a variety of physical variables of different types and dimensions. These physical variables should be transformed to neuronal variables. Hence, sensory acquisition and processing must employ a variety of transformations. The first transformations occur already at the level of the sensory receptors during transduction. These transformations are implemented by a variety of closed loops, mostly at the molecular and

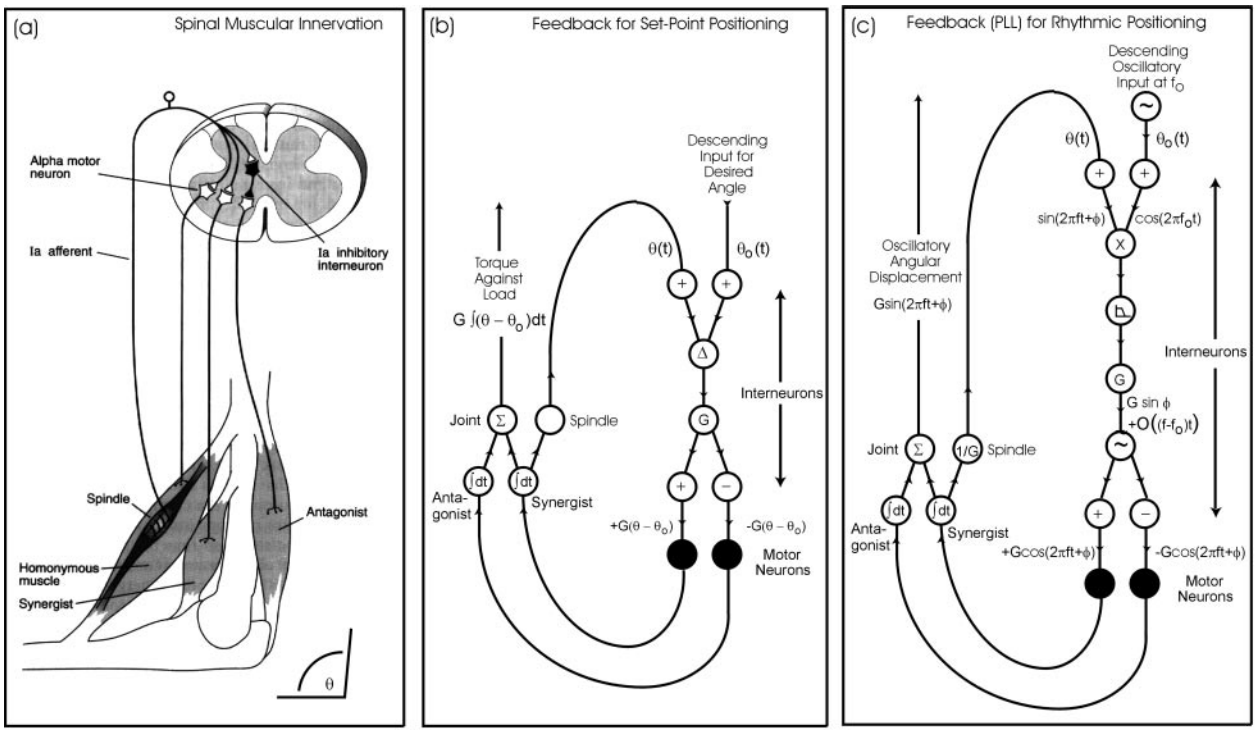

Figure 2. Two possible aspects of feedback control in the spinal innervation of the muscles in a joint. (*a*) Diagram of the spinal circuit that incorporates feedback from muscle spindles, which code displacement. The motor neuron output is to both synergistic as well as antagonistic muscles. Feedback via spindles in the synergistic muscle fibers reports a monotonic function of the joint angle. Descending input (not shown) occurs onto both motor neurons and interneurons. Figure abstracted from Kandel, Schwartz and Jessel (Gordon, 1991). (*b*) Functional scheme for plausible feedback control of set-point positioning. Feedback is via proprioception. Elements of the circuit are labeled with their function, i.e. +, Δ and *G* refer to interneurons with excitatory output that are used for unity gain, differencing and gain, respectively, and '–' refers to interneurons with inhibitory output. The muscles are taken to perform temporal integration of their inputs and the joint to perform a sum function, Σ, of the torques produced by the synergistic and antagonistic muscles. (*c*) Functional scheme for possible feedback control of rhythmic output. This scheme illustrates the architecture of a phase-locked loop for rhythmic output generation. An input-controlled internal oscillator, denoted by '~', is locked to the desired frequency, f_0. Elements of the circuit are labeled with their function, as in part (*a*), with the addition that 'X' refers to the multiplication or mixing of two signals and the boxed Bode plot refers to the low-pass filtering of the signal. The basic forms of the sinusoidal signals are further indicated. At lock, the actual frequency, *f*, equals the desired frequency, f_0, and the input to the controlled oscillator is a constant drive term equal to $G\cos\phi$.

cellular levels. Later transformations usually transform feature-based codes to more abstract codes that are used for integration and motor control.

Closed-loop Computations in the Vibrissa Sensorimotor System

Rats whisk as they probe their immediate environment for the presence of objects, obstacles, or food. Animals can also be trained to whisk in air, in the absence of tactile or visual input. We refer to this as 'free whisking'. It consists of large back-and-forth movements that subtend as much as 100° (Fig. 3*a*) and persist for bouts up to 4 s. Interestingly, animals will whisk at essentially a constant frequency over the entire period of the bout, as seen in the rectified mystatial electromyogram (EMG) (Fig. 3*b*), a measure of vibrissa position. They can then whisk again at the same or a different frequency, but again hold the frequency constant (Fig. 3*c*) (Berg and Kleinfeld, 2002). Thus, whisking appears to be driven by an accurate pacemaker, with a frequency that varies between whisking bouts, but that is constant within a bout, or alternatively, different pacemakers control whisking at different bouts. The distribution of the whisking frequencies generally lies between 5 and 15 Hz (Fig. 3*d*) and the spectral purity of the whisking is independent of frequency. The accuracy of whisking within each bout is suggestive of phase-sensitive detection as a decoding scheme of vibrissae position (Kleinfeld *et al*., 1999). This decoding can, in principle, be accomplished by open or closed loops (Ahissar, 1995, 1998; Ahissar *et al*., 1997).

The vibrissa sensorimotor system contains several circuits, parallel and embedded in each other, that close the loop between the sensory receptors that are activated by vibrissa deflections and the muscles that move the vibrissae (Kleinfeld *et al*., 1999). This system also contains feedback loops that enclose various processing stations (i.e. sensory thalamus and cortex) within closed anatomical loops. Is local computation between these stations dominated by feedforward or closed-loop dynamics? With feedforward processing, sensory signals should propagate to the cortex via brainstem and thalamic 'relay' neurons. Thus, vibrissa-locked activities of somatosensory cortical neurons should lag whisking activity. However, during epochs of vibrissa-locked oscillatory activity in freely behaving rats (Fee *et al*., 1997), as well as in awake restrained rats (Brecht and Sakmann, 2001), cortical neurons show a full range of phase relations relative to the angle of the vibrissae. Further, in awake rats, the phase of thalamic oscillatory activity lags the phase of both brainstem and cortical activity (Nicolelis *et al*., 1995). While inconsistent with a feedforward scheme, these observations are consistent with a closed-loop computation scheme, in which cortical oscillatory activity is not driven by sensory events but is generated independently in the cortex and is used to decode, or to 'measure', the input periodicity.

The existence of a central mechanism that 'measures' the input periodicity was proposed by Mountcastle and colleagues in the 1960s to explain their observations from the primate somatosensory system (Talbot *et al*., 1968). The possibility that

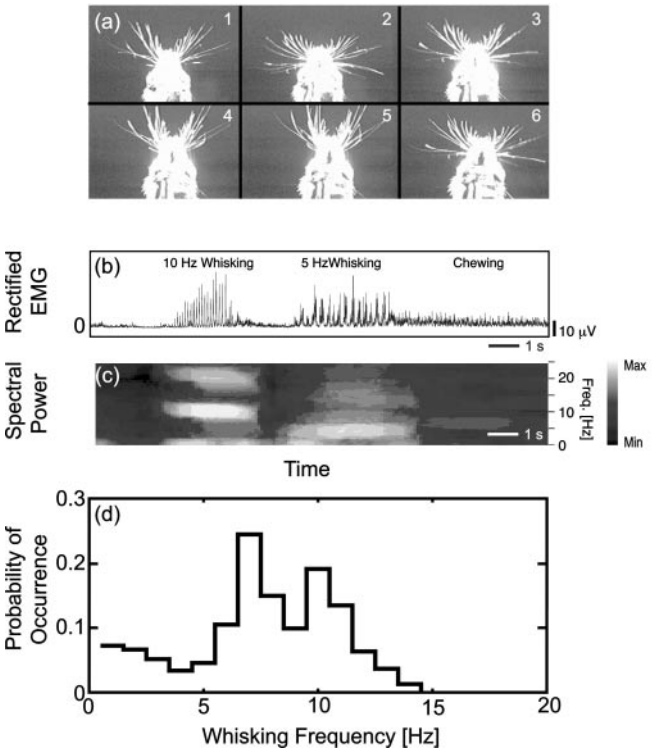

Figure 3. Fundamental aspects of free whisking. (*a*) Sequential videographs of a rat whisking freely in air. The images were obtained at 60 frames/s. The rat is searching for a food tube with its vibrissae while blindfolded. Figure from supplemental data for Fee *et al.* (Fee *et al.*, 1996). (*b,c*) Time-series and accompanying spectrogram of the electromyogram (EMG) of the intrinsic muscles in the mystatial pad as an animal whisks in air. Note the two whisking bouts, each with a different but steady whisking frequency, as well as the period of low amplitude chewing. Data from O'Connor *et al.* (O'Connor *et al.*, 2002). (*d*) Distribution of whisking frequencies taken from 232 whisking epochs in one animal. Figure derived from EMG data in O'Connor *et al.* (O'Connor *et al.*, 2002).

such a mechanism exists in rats was investigated by testing the predictions of several potential mechanisms in anesthetized rats (Ahissar *et al.*, 1997, 2000, 2001a; Sosnik *et al.*, 2001) and is reviewed elsewhere (Ahissar and Arieli, 2001; Ahissar and Zacksenhouse, 2001). The results of these experiments suggest that one of the two major thalamocortical systems, the paralemniscal system, contains many parallel loops that function as phase-locked loops (PLLs). A PLL is an algorithm for temporal processing with periodical signals, discovered by electrical engineers in the 1930s (Bellescize, 1932) and is considered to be an optimal temporal decoder. It can be implemented by software, electronic circuits (Gardner, 1979), single neurons (Hoppensteadt, 1986), or neuronal circuits (Ahissar and Vaadia, 1990; Ahissar, 1998). The elegance of the PLL emerges mainly from its adaptive operation, which is a direct outcome of its closed-loop design (Gardner, 1979; Ahissar, 1998; Kleinfeld *et al.*, 1999). One implementation of a PLL was presented above to describe motor control of the skeletal joint (Fig. 2*c*). Other neuronal implementations of PLLs could, in principle, occur all over the nervous system. In particular, a sensory PLL for decoding vibrissal temporally encoded information could be implemented across thalamocortical loops, by using cortical oscillators, cortical inhibitory neurons and thalamic 'relay' neurons, where the last are hypothesized to function as phase detectors (Fig. 4) (Ahissar *et al.*, 1997; Ahissar and Arieli, 2001; Ahissar and Zacksenhouse, 2001). For such implementations, which consist entirely of spiking neurons, discrete-time representations are probably more appropriate than continuous-time representations (Ahissar, 1998). This is particularly true for the vibrissal system, in which computations involve neurons that fire one or few spikes per whisking cycle.

Decoding by PLLs: Theory, Predictions and Tests

In principle, a single PLL can perform temporal decoding over a significant range of input frequencies. However, our data suggest that many PLLs operate in parallel within the paralemniscal thalamocortical system. The existence of many PLL circuits in parallel is conjectured from two observations. First, neurons in sensory (Fee *et al.*, 1997) as well as motor cortex (Kleinfeld *et al.*, 2002) are locked to motion of the vibrissa over the full range of phases, 0 to 2π, in the awake, whisking animal. Second, many independent cortical oscillators exist in the somatosensory cortex of anesthetized rodents, each exhibiting a different spontaneous frequency and each oscillating independently from the others when no sensory stimulus is applied (Ahissar *et al.*, 1997) [see also (Ahissar and Vaadia, 1990; Schoner *et al.*, 1992)]. This parallel-processing scheme entails specific predictions – predictions that emerge from the PLL equations.

The equations of a discrete form of a linear PLL (Fig. 4), in the absence of noise, are:

$$R_{out}(n) = R - \alpha\tau_D(n) \quad (1)$$

$$\tau_D(n+1) = \tau_D(n) + T_o(n) - T_i(n+1) \quad (2)$$

where n indexes the whisking cycle, $R_{out}(n)$ is the output, measured in spike-counts, of the PLL at cycle n, R is the output spike-count when $\tau_D = 0$, α is a constant, and $\tau_D(n)$ is the temporal delay between the two inputs, t_{osc} and t_{bs} (Fig. 4) to the phase detector, and is given by:

$$\tau_D(n) = t_{osc} - t_{bs} \quad (3)$$

$T_i(n)$ is the period (1/frequency) of the input, and $T_o(n)$ is the period of the oscillator. The latter period is given by

$$T_o(n) = T_c + \gamma R_{out}(n) \quad (4)$$

where T_c is the intrinsic period of the oscillator, i.e. the period with which the oscillator should oscillate if it would receive no input, and γ is a constant.

At steady-state, $\tau_D(n+1) = \tau_D(n)$ and thus the PLL is locked [$T_o = T_i$, in equation (2)] and, from equations (1) and (4),

$$\tau_D = R/\alpha + (T_c - T_i)/G \quad (5)$$

where $G = \alpha\gamma$ is the 'open-loop gain' of the circuit.

Thus, with linear PLLs at steady-state, τ_D is linear with respect to the term $(T_c - T_i)$. The latency of the cortical oscillator ($t_{osc} - t_{stim}$, where t_{stim} is stimulus onset time) equals, from equation (3):

$$t_{osc} - t_{stim} = \tau_D + (t_{bs} - t_{stim}) \quad (6)$$

and the latency of the phase detector's output equals

$$t_{pd} - t_{stim} = \tau_D + (t_{bs} - t_{stim}) + D_{pd} \quad (7)$$

where D_{pd} is the input–output delay (including conduction delays) of the phase detector. Thus, thalamic and cortical latencies equal τ_D + constant. This relationship, together with equation (5), provides several testable predictions.

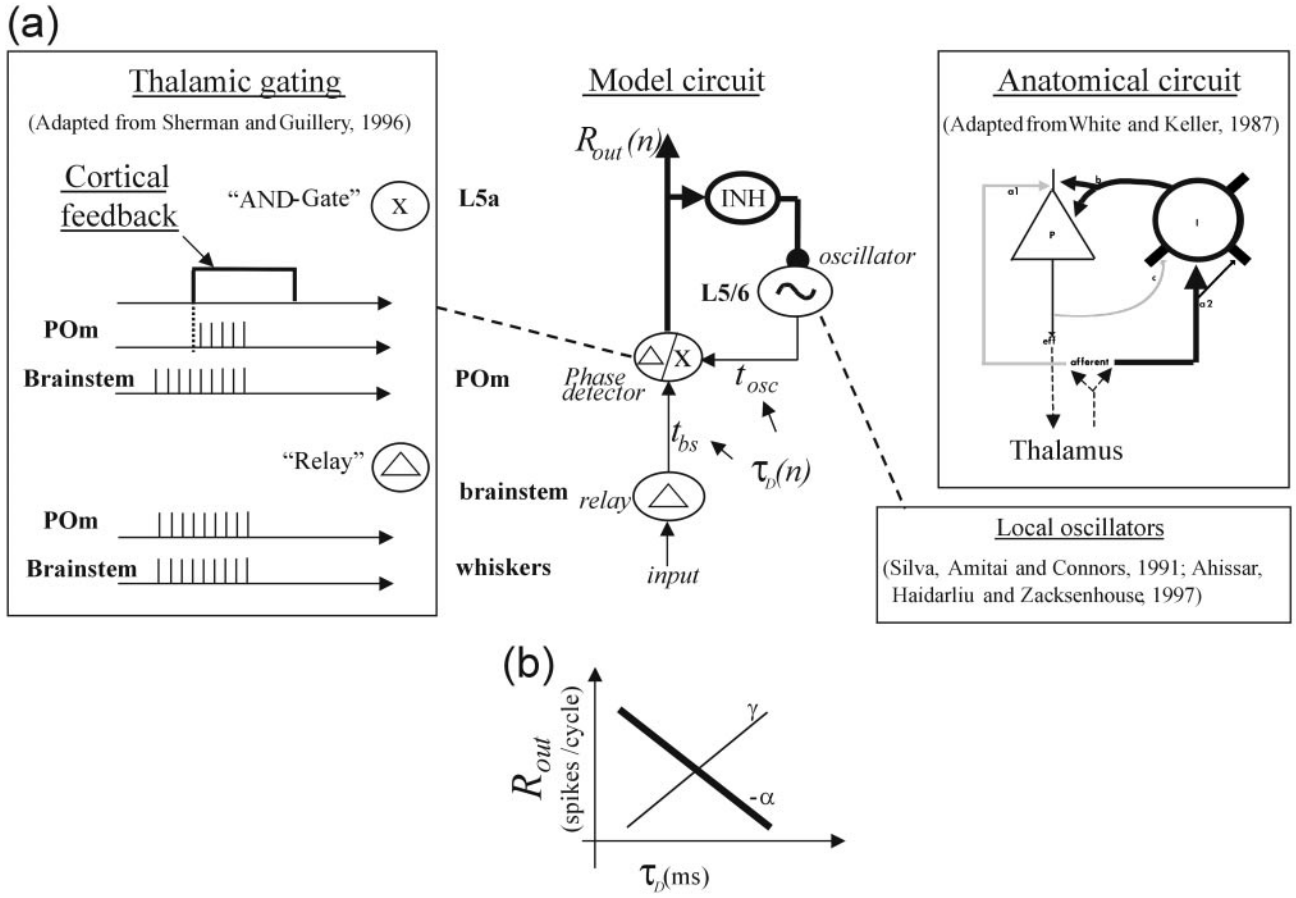

Figure 4. Model of thalamocortical PLL. (*a*) The model circuit is a composite of independent anatomical and physiological data. The connections in the model circuit are those anatomical connections that exist in the vibrissal thalamocortical system and are required for a PLL operation. These connections are re-plotted in black ('Anatomical circuit', right panel) in the thalamocortical circuit proposed by White and Keller (White and Keller, 1987); the connections that are not essential for a PLL operation are plotted in gray. The thalamic neurons are assumed to switch between 'Relay' and 'AND gate' modes ('Thalamic gating', left panel), as suggested by Sherman and Guillery (Sherman and Guillery, 1996). In relay mode, thalamic neurons transfer the input from the brainstem 'as is'. In AND-gate mode, thalamic neurons transfer only that portion of the input for which the timing overlaps with the cortical feedback. The cortical feedback to the thalamus is dominated by cortical local oscillators, such as those described in earlier work (Ahissar and Vaadia, 1990; Silva *et al*., 1991; Ahissar *et al*., 1997). The feature of the local oscillators which is critical for the PLL algorithm is the ability of these neurons, once fired, to fire again after an intrinsically determined period. Thus, after firing a spike (or burst), they will tend to fire another spike (burst) after a given interval (T_c) even if not stimulated. This interval can be increased by inhibition and decreased by excitation (Perkel *et al*., 1964; Silva *et al*., 1991; Ahissar *et al*., 1997). Connections carrying temporal coding are plotted by thin lines and those carrying spike-count coding are plotted by thick lines. The oscillator transforms spike-count to temporal code and the phase detector transforms temporal to spike-count code. $\tau_D(n) = t_{osc}(n) - t_{bs}(n)$ is the temporal delay between the two inputs to the POm, where t_{bs} is the onset time of the brainstem burst, t_{osc} is the onset time of the feedback burst and n is the index of the whisking cycle. $R_{out}(n)$ is the spike-count of the POm output. The model scheme is from earlier work (Ahissar, 1998). (*b*) Schematic transfer functions for a linear PLL. The thin curve is the transfer function of the oscillator; the thick curve is the transfer function of the phase detector; γ and α are the gains of the oscillator and phase detector, respectively.

The first prediction is that steady-state response latencies, in thalamus and cortex, should increase with increasing input frequencies [$f_i = 1/T_i$; for any given T_c, τ_D will increase with decreasing T_i, see equation (5)]. This was indeed observed in the thalamic and cortical stations of the paralemniscal system, i.e. POm and layer 5a, respectively (Ahissar *et al*., 2000). The steady-state response phases of POm and layer 5a neurons increase with the stimulus frequency (Fig. 5*a*). The response phases increase not only due to the decreased stimulus period, but also due to an explicit increase in response latencies, as demonstrated by the distributions of onset latencies among these neurons (Fig. 5*b*).

The second prediction derived from equation (5) is that, when the input frequency is constant, the spread of thalamocortical latencies should be determined by the spread of the intrinsic periods (T_c) of cortical oscillators. The periods T_c cannot be measured *in vivo*, since the oscillators always receive inputs as a consequence of spontaneous activity. Nevertheless, to the extent that the spontaneous drive is similar across different recordings, the spread of spontaneous oscillations may provide an approximation to the spread of T_c. Spontaneously oscillating neurons, which could potentially function as oscillators in vibrissa-related PLLs, have been previously recorded in anesthetized rats and guinea pigs (Ahissar *et al*., 1997). To test the above prediction, we re-plotted the frequency distribution of the rat oscillating neurons as a period distribution, in the range that is relevant for decoding whisking frequencies (Fig. 5*c*, black broken curve). With the PLL scheme described above, T_c should be smaller than the maximal decodable T_i. Thus, to cover the range of spontaneous oscillatory periods which could be relevant for decoding whisking frequencies, we depicted periods $20 < T_{spont} < 120$ ms, corresponding to frequencies between ~8 and 50 Hz. Within this range, the distribution of spontaneous oscillating periods contains a mode whose spread approximates that of response latencies in POm and Layer 5a (Fig. 5*c*), as predicted by the PLL model. This mode contains spontaneous oscillatory

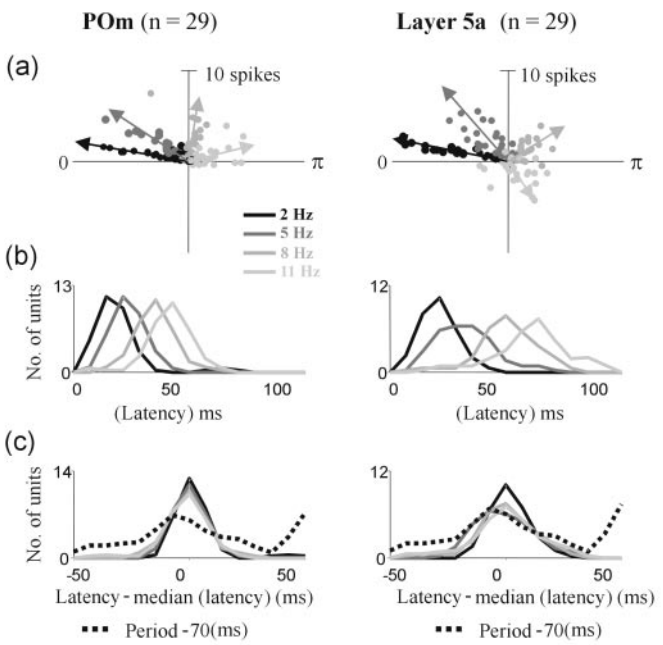

Figure 5. Spread of latencies, phases and oscillating periods during vibrissa stimulation in the anesthetized rat. Recordings were made from 29 units of the POm and 29 units of layer 5a of the barrel cortex. (*a*) Polar plots of phases and spike-counts (per cycle) for four stimulation frequencies (2, 5, 8 and 11 Hz; gray level decreases with frequency). Stimulations were air-puffs to groups of vibrissae containing receptive fields of the neurons. Radial dimension encodes spike-count per cycle and circular dimension encodes phase (= 2π latency/stimulus period). The arrows point to the vector average (with magnitude multiplied by four). Data are from earlier work (Ahissar *et al.*, 2001a; Sosnik *et al.*, 2001). (b) Distributions of response latencies (to 0.5 of response peak) of the same data as in (*a*). (*c*) Distributions of response latencies as in (*b*), plotted around their median values for each latency (solid curves) and distribution of cortical oscillating periods plotted around period = 70 ms (broken curve). Data of oscillating periods are from earlier work (Ahissar *et al*., 1997).

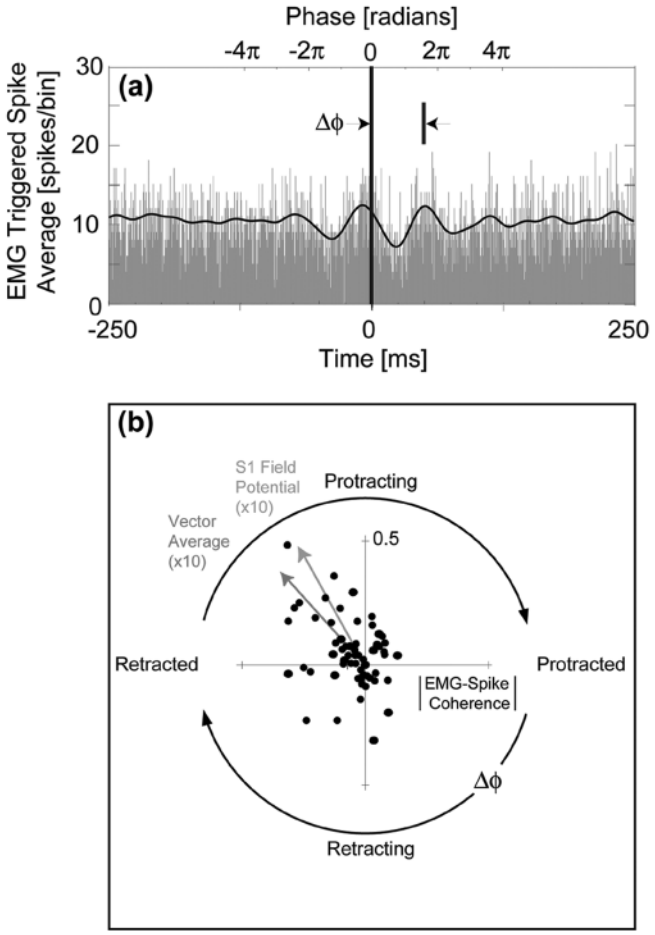

Figure 6. The modulation of spiking in vibrissa S1 cortex by rhythmic whisking in air. (*a*) Illustration of electromyogram (EMG) triggered spike rate. The modulation of the spike rate shows that the output of this unit is modulated by whisking. Data are from earlier work (Fee *et al.*, 1997). (*b*) Distribution of the magnitude and phase of the spectral coherence between cortical spiking and the mystatial EMG. The average whisking frequency was 9 Hz, with a range of ± 2 Hz. The arrows (with magnitude multiplied by 10) point to (i) the vector average and (ii) the coherence inferred from differential local field potential (LFP) data. Note the strong correspondence between the two averaging techniques. Data are from earlier work (Fee *et al.*, 1997; O'Connor *et al.*, 2002).

periods between 50 and 105 ms, corresponding to frequencies between 9.5 and 20 Hz. The striking overlap between the spread of T_c and that of τ_D (Fig. 5*c*) could be interpreted to imply that the hypothetical thalamocortical PLLs function near their linear regime – equation (5).

According to the above results, temporal decoding in the paralemniscal system is accomplished by sets of many parallel thalamocortical PLLs, each with a different working range, i.e. a range of input frequencies that can be decoded by that PLL. If this is the case, then during natural whisking the spread of cortical phases should exhibit the accumulation of the spreads of cortical T_cs and of whisking frequencies. This is consistent with cortical data from freely moving rats (Fee *et al.*, 1997). Cortical neurons phase-lock to whisking movements with different phases (Fig. 6). While the ensemble vector has a phase of about $\pi/4$ relative to the retracted phase of the mystacial EMG activity, the entire population of single units cover the entire range of possible phases (Fig. 6b). The cortical phase distribution observed during free whisking (Fig. 6*b*) resembles that observed in anesthetized rats during vibrissa stimulation at whisking-range frequencies, i.e. frequencies between 5 and 11 Hz (Fig. 5*a*, right panel, gray dots). In both cases, response phases distribute between 0 and 2π and response magnitudes are larger at low response phases, consistent with the PLL model.

Thus, during whisking, cortical neurons phase-lock to vibrissa movement at different phases (Fig. 6*b*), perhaps based on their specific loop affiliation. As described above, we speculate that, for every neuron, its response phase lag depends on the intrinsic period (T_c) of the oscillator driving the loop containing that neuron. If this is the case, these phase lags contain information about the whisking frequency. The same information can be extracted from the spike-counts of cortical neurons. Both signals are likely to be noisy at the cortical level and the system may combine both sources of information to improve the fidelity of the representation of the whisking frequency. To compute the phase lag, the exact reference of whisking onset time has to be available. This suggests a possible role for the lemniscal system, in addition to its other functions, within this temporal decoding scheme: the lemniscal system, which responds at a fixed latency at all frequencies within the whisking range (Hartings and Simons, 1998; Ahissar *et al.*, 2001a; Sosnik *et al.*, 2001), can provide the required reference signal. Comparison of the outputs of the lemniscal and paralemniscal systems, say at layer 2/3 of the cortex (Ahissar *et al.*, 2001a), can provide a measure of the desired phase-lag. Further, the reference signal conveyed by the lemniscal system might be useful in computing the contact angle when the vibrissae touch an object during protraction.

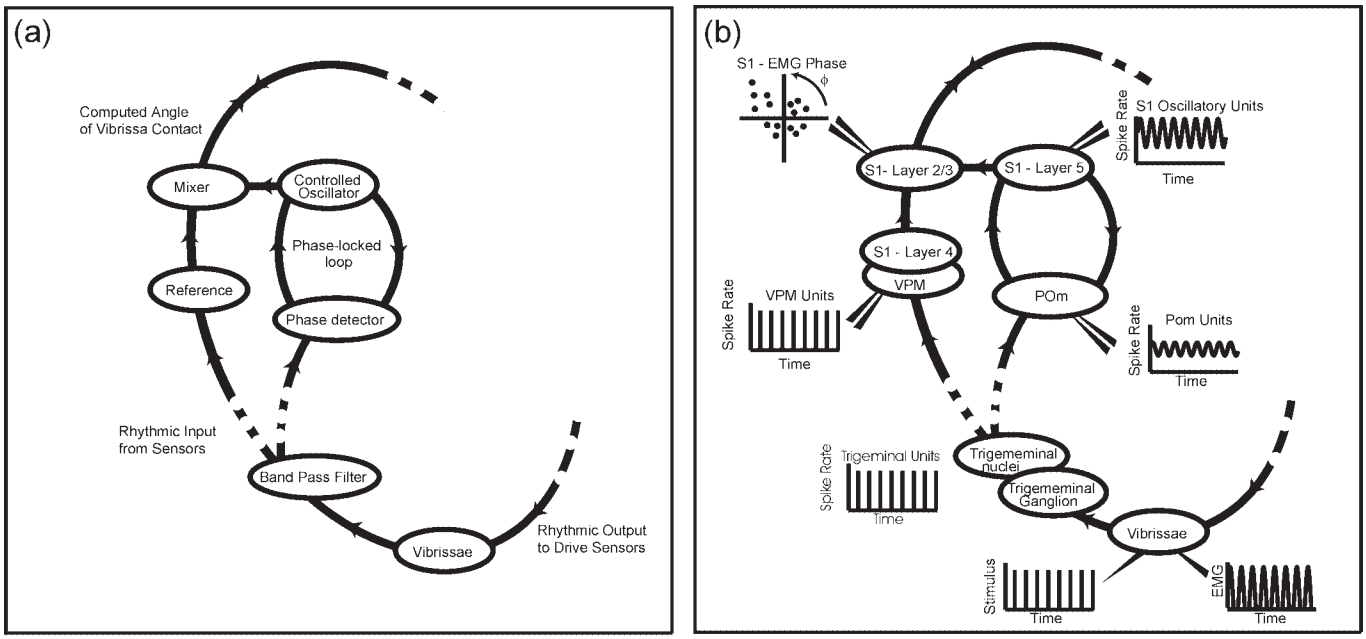

Figure 7. A schematic description of early stages in vibrissal temporal decoding. The functional block diagram (*a*) and proposed implementation (*b*) of a plausible computational scheme are depicted. The sensory input captured by the vibrissae receptors, either during whisking or external stimulation, is conveyed to the two thalamic nuclei: VPM and POm. The loops are composed of neurons from POm and from layers 5 and 6 of S1, which together function as phase-locked loops (see Fig. 4). VPM and layer 4 neurons convey a reference signal. Outputs of both streams are 'mixed' in layer 2/3 of the cortex to extract the frequency out of the phase difference.

Thus, an outline of the first stages of the temporal decoding scheme can look like that depicted schematically, and in abstract form, in Figure 7. Note that (i) the paralemniscal loop in fact contains many loops in parallel and (ii) only lemniscal signals that relate to this computation are depicted, ignoring other, parallel, lemniscal processes.

Further Predictions for Thalamocortical PLLs

Critical tests of the PLL hypothesis should involve measurements with behaving rats. If thalamocortical loops function as PLLs during tactile exploration, it is predicted that in the exploring rat:

1. paralemniscal (POm and layer 5a in the barrel cortex) latencies should increase with increasing whisking frequencies;
2. paralemniscal spike-counts (per cycle) should decrease with increasing whisking frequencies;
3. during protraction, contacts at more anterior positions will be represented by larger paralemniscal spike-counts.

The last prediction depends on the actual set point of the thalamocortical PLLs and thus is not a critical prediction (Ahissar, 1998; Kleinfeld *et al.*, 1999). Yet, the data collected so far indicate thalamocortical set points for which such a dependency is expected (Ahissar *et al.*, 1997; Ahissar and Arieli, 2001).

Possible Alternative Mechanisms

Closed-loop mechanisms in general and PLL in particular, are certainly not the only possible mechanisms for processing whisking-related information. Feedforward mechanisms could also decode the temporally encoded information generated during vibrissa movement (Ahissar, 1995; Buonomano and Merzenich, 1995). The data we collected, however, are inconsistent with such feedforward mechanisms (Ahissar and Arieli, 2001).

Another possibility is that vibrissa position is not encoded by temporal cues. For example, different ganglion or brainstem neurons might be associated with different phases along the whisking path, such that the identity of the activated neuron indicates the position (angle) of the vibrissa (a 'labeled-line' coding scheme). Or, alternatively, population of neurons might encode vibrissa position in their ensemble firing rate. Unfortunately, a systematic investigation of the encoding of vibrissa position during whisking has yet to be made. The existing data about stimulus encoding by neurons of the trigeminal ganglion were collected during electrical stimulations of the motor nerve (Zucker and Welker, 1969) and during passive mechanical deflections of the vibrissae (Gibson and Welker, 1983; Lichtenstein *et al.*, 1990; Shoykhet *et al.*, 2000). In these data, there are no signs of a labeled-line code as described above. Yet, a population rate code might be constructed from neurons exhibiting directional and amplitude dependency (Zucker and Welker, 1969; Gibson and Welker, 1983; Shoykhet *et al.*, 2000).

Sensorimotor Servo Loop

Motivated by the accumulating data presented above and by the analogy between the vibrissa system and other sensorimotor systems (Ahissar, 1998), we propose that the entire sensorimotor loop of the vibrissal system functions as a servo loop, whose controlled variables are not external, as in the case of the stick angle in Wiener's example, but are, rather, internal. Unlike motor servo control, the purpose of the sensorimotor servo control is to optimize sensory computation, much like automatic gain control loops optimize decoding in radio receivers. Several schemes of sensorimotor servo loops could accomplish optimization of sensory processing. We delineate here two such schemes.

The first servo scheme is aimed at stabilizing the whisking

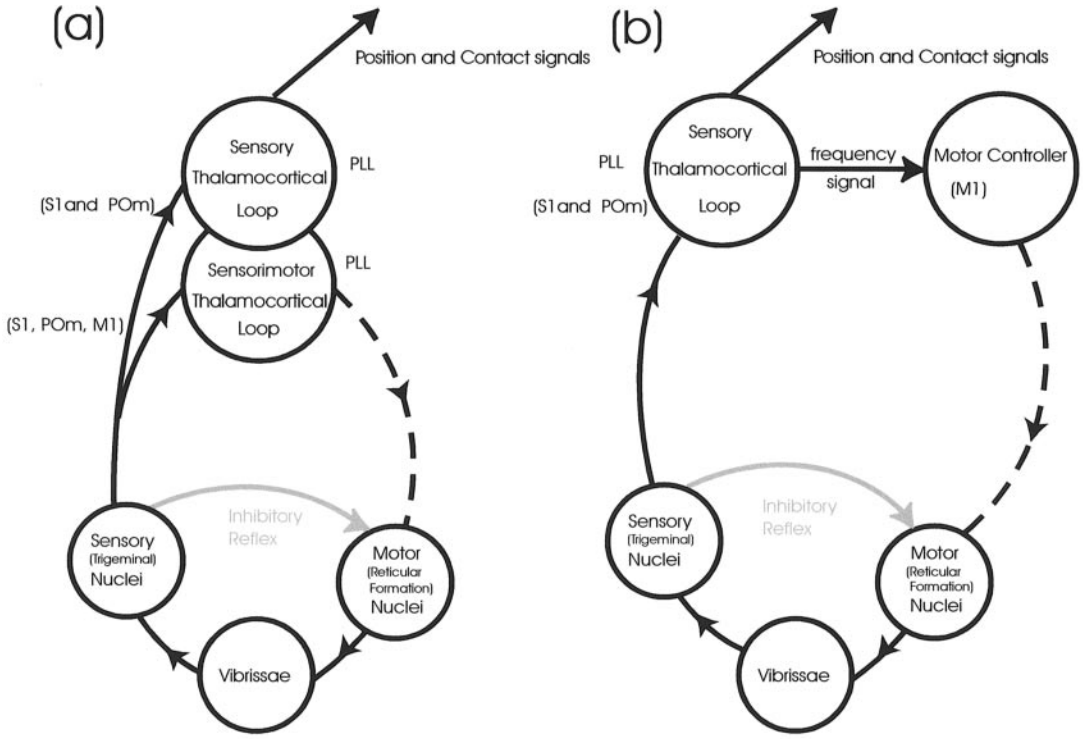

Figure 8. Possible servo-loop schemes for the vibrissa sensorimotor system. Two possible schemes are depicted; only essential components are shown for clarity. (*a*) Two thalamocortical loops function as PLLs. One, composed by S1 and POm neurons, accomplishes only sensory computations (of vibrissa position and object location) and is not involved in sensorimotor operation. The other, composed of S1, POm and M1 neurons, extracts the fundamental input frequency, a signal that is used to stabilize whisking frequency via a servo loop. (*b*) One thalamocortical PLL is used for both sensory computations and control of whisking frequency within the sensory-motor servo loop.

frequency in the presence of contact of the vibrissae with objects. As demonstrated by the data in Figure 3, the whisking frequency is stable during each whisking bout. A stable whisking frequency facilitates phase-sensitive sensory computation and thus might be actively maintained by a sensory-motor servo loop (Fig. 8*a*), consisting of another set of PLLs, implemented across S1, M1 and POm. Experiments on the sensory response of neurons in vibrissa M1 cortex in awake animals (Kleinfeld *et al.*, 2002) indicate that M1 neurons compute the fundamental frequency of a complex, repetitive input. The interpretation of this and related results could be that vibrissa S1 cortex and M1 cortex, together with the POm, are part of a PLL that extracts the fundamental frequency of the input and maintains a stable frequency of whisking.

Sensorimotor servo loops could also serve directly at optimizing sensory processing, by controlling the set-points of the sensory (thalamocortical) PLLs (Fig. 8*b*). Naturally, the optimal set-point for a given loop is located at the center of its working range, since in that condition the loop can handle the largest input modulations (Ahissar, 1998). Thus, if vibrissal temporal decoding were accomplished by a single thalamocortical PLL, the role of the sensorimotor servo loop would be to maintain the set-point of this PLL at the center of its working range. Since the set-point of the PLL is determined by the average input frequency (Ahissar, 1998), maintaining the optimal set-point is accomplished by controlling whisking frequency. The 'error signal', whose value determines the motor output, should be one of the variables composing the PLL's set-point, namely spike-count or latency of thalamic or cortical neurons. Of the two, the spike-count variable is more reliable (Ahissar *et al.*, 2001a; Sosnik *et al.*, 2001) and is probably more suitable for controlling motor activity (Georgopoulos, 1986; Wessberg *et al.*, 2000).

In the real brain, closed-loop optimization is complicated by processing in parallel channels. According to the results described above, temporal decoding in the paralemniscal system is accomplished by sets of many parallel thalamocortical PLLs, each possessing a different working range. Although the working range of any single PLL is limited (Ahissar, 1998), a collection of PLLs, each having a slightly different working range, can decode the entire required frequency range. However, such a scheme poses serious challenges to the system. For example, for a given input frequency, different PLLs will produce different output values, depending on their T_c. Thus, for the same input, some pools of PLLs will produce meaningful outputs while others, which will be driven out of their working ranges, will produce nonsense outputs. How can the readout circuit isolate the 'proper' PLLs, namely those PLLs whose output is relevant for sensory computation during the performance of a given task? A solution to this problem might be 'built-in' the sensorimotor servo loop scheme. By maintaining the whisking frequency centered on a given frequency, the servo loop in fact selects a range of PLLs whose optimal set-points, i.e. centers of their working ranges, are at that frequency. These 'relevant' PLLs will present full range modulations of their output values while other, 'non-relevant', PLLs will exhibit limited modulations due to saturation. Both readout circuits and motor control circuits should be able to tune to the PLLs that exhibit the largest modulations. By this tuning, the sensorimotor servo loop converges to its own set-point, which is thus determined by the whisking frequency and the profile of activity modulations across thalamocortical PLLs.

The set-point of the sensorimotor loop depends on the task in hand. For example, object localization, which involves low spatial (and thus also temporal) frequencies, should lead to set-points optimal for low-frequency PLLs. In contrast, fine texture analysis, which usually involves high spatial and temporal frequencies, should lead to set-points optimal for high-frequency PLLs.

In the above two examples, the motor variable used by the servo loop was the whisking frequency. This is not the only available variable for servo control. Other variables, such as protraction velocity or amplitude, can be used as well. For example, when scanning a textured surface, protraction velocity (V) might be controlled to optimize the temporal frequency (f) and compensate for changes in the texture's spatial frequency (SF), since $f = |V| * SF$. It would probably be reasonable to assume that whisking frequency is usually the variable used to optimize processing by paralemniscal PLLs, whereas protraction velocity is used to optimize processing by lemniscal PLLs, if they exist. This is because paralemniscal PLLs are tuned to whisking frequencies, which peak near 10 Hz (Fig. 3*d*), whereas lemniscal PLLs are probably tuned to higher frequencies, which are produced while scanning textures and determined by protraction velocity.

Predictions for the Servo Loop

A major potential function of a sensorimotor servo loop is thus to maintain optimal conditions for sensory processing (see second example above). A straightforward prediction of such a loop is that motor variables of whisking should depend on the stimulus and the task at hand, in a way that optimizes sensory processing. For example, with texture identification or discrimination, whisking velocity should depend on the texture's spatial frequency such that the resulting temporal frequency is maintained within the working range of the sensory PLLs. Usually, this will require a reduction of velocity when the spatial frequency increases and vice verse.

Another prediction of the sensorimotor servo loop is that if sensory information is removed, by some lesion that 'opens the sensorimotor loop', the motor system will not be able to maintain a constant whisking profile against changing conditions, such as changes in air pressure or object profiles. Moreover, under these conditions, the motor system might drive the vibrissae to whisk at one of the extreme states: either with maximal or with minimal possible frequency.

Concluding Remarks

What is the neural code? The lack of an accepted answer to this question seems to significantly hamper understanding of brain operation. But is this question well-posed? Is there only one neural code for the brain? As can be judged from the large repertoire of potential neural codes observed during neuronal recordings in various brain regions and in various conditions, this does not seem to be the case. The brain does not seem to use a single, unified neural code for all its processes. Rather, each process, and each interaction between processing stations, probably involves specific neural codes. Moreover, a neural process can even convert one code to another. Thus, instead of 'what is the neural code?', a more relevant question for understanding the brain seems to be 'what are the neural processes?'. As Perkel and Bullock put it more than 30 years ago, 'The problem of neural "coding" is that of elucidating the transformations of information effected by the nervous system' (Perkel and Bullock, 1968).

Neuronal processes that are implemented by single neurons, such as transduction, conduction, filtering and integration, have been described through the years. Processes implemented by neuronal circuits have also been described. Among these are feedforward transformations and recurrent relaxation by neural networks, oscillations by excitatory–inhibitory loops, and motor control by closed loops. To this repertoire we add here sensory computation by closed loops. We suggest that a significant portion of sensory processing is implemented by closed-loop computations. We have shown here how thalamocortical phase-locked loops may decode information that is encoded in time by the rat vibrissae and how such loops could be nested within a larger-scale sensory-motor servo loop. Similar phase-locked loops might operate in the visual (Ahissar and Arieli, 2001) and auditory (Ahissar *et al*., 2001b) systems to decode temporally encoded information.

Much of our understanding of the operation of neural networks comes from physics. Similarly, understanding closed-loop computation should benefit from engineering. Engineers discovered that closed loops often provide extremely elegant solutions for 'real-world' problems, the same kind of problems with which living brains are routinely challenged. Yet, engineered closed loops usually lack one important feature, which is inherent in brains: built-in plasticity. It is possible that closed-loop computation and plasticity are two of the most critical features which make brains so efficient. Achieving an understanding of the interplay between closed-loop computations and plasticity is a further challenge.

Notes

We thank Per M. Knutsen and Marcim Szwed for their helpful comments on the manuscript, and the Institute for Theoretical Physics (ITP), University of California at Santa Barbara, for its hospitality. This work was supported by the United States–Israel Binational Science Foundation (grant 2000299 to E.A.), the Abramson Family Foundation (grant to E.A.), the Nella and Leon Benoziyo Center (grant to E.A.), the National Institutes of Mental Health (grant MH59867 to D.K.) and the National Science Foundation (grant PHY99-07949 to the ITP).

Address correspondence to Ehud Ahissar, Department of Neurobiology, The Weizmann Institute of Science, Rehovot 76100, Israel, email: ehud.ahissar@weizmann.ac.il, or to David Kleinfeld, email: dk@physics.ucsd.edu.

References

Ahissar E (1995) Conversion from temporal-coding to rate-coding by neuronal phase-locked loops. The Weizmann Institute of Science: Technical Report GC-EA/95-4.

Ahissar E (1998) Temporal-code to rate-code conversion by neuronal phase-locked loops. Neural Comput 10:597–650.

Ahissar E, Arieli A (2001) Figuring space by time. Neuron 32:185–201.

Ahissar E, Vaadia E (1990) Oscillatory activity of single units in a somatosensory cortex of an awake monkey and their possible role in texture analysis. Proc Natl Acad Sci USA 87:8935–8939.

Ahissar E, Zacksenhouse M (2001) Temporal and spatial coding in the rat vibrissal system. Prog Brain Res 130:75–88.

Ahissar E, Haidarliu S, Zacksenhouse M (1997) Decoding temporally encoded sensory input by cortical oscillations and thalamic phase comparators. Proc Natl Acad Sci USA 94:11633–11638.

Ahissar E, Sosnik R, Haidarliu S (2000) Transformation from temporal to rate coding in a somatosensory thalamocortical pathway. Nature 406:302–306.

Ahissar E, Sosnik R, Bagdasarian K, Haidarliu S (2001a) Temporal frequency of whisker movement. II. Laminar organization of cortical representations. J Neurophysiol 86:354–367.

Ahissar E, Nagarajan S, Ahissar M, Protopapas A, Mahncke H, Merzenich M (2001b) Speech comprehension is correlated with temporal response patterns recorded from auditory cortex. Proc Natl Acad Sci USA 98:13367–13372.

Ahrens KF, Levine H, Suhl H, Kleinfeld D (2002) Spectral mixing of rhythmic neuronal signals in sensory cortex. Proc Natl Acad Sci USA (in press).

Amit D (1989) Modeling brain function. New York: Cambridge University Press.

Bellescize H de (1932) La reception synchrone. Onde Electr 11:230–240.

Ben-Yishai R, Bar-Or RL, Sompolinsky H (1995) Theory of orientation tuning in visual cortex. Proc Natl Acad Sci USA 92:3844–3848.

Berg RW, Kleinfeld D (2002) Rhythmic whisking by rat: retraction as well as protraction of the vibrissae is under active muscular control. J Neurophysiol (in press).

Brecht M, Sakmann B (2001) Whole-cell recordings in rat somatosensory cortex during whisking episodes. Soc Neurosci:130.135.

Buonomano DV, Merzenich MM (1995) Temporal information transformed into a spatial code by a neural network with realistic properties. Science 267:1028–1030.

Fee MS, Mitra PP, Kleinfeld D (1997) Central versus peripheral determinants of patterned spike activity in rat vibrissa cortex during whisking. J Neurophysiol 78:1144–1149.

Gardner FM (1979) Phaselock techniques. New York: John Wiley.

Georgopoulos AP (1986) On reaching. Annu Rev Neurosci 9:147–170.

Gibson JM, Welker WI (1983) Quantitative studies of stimulus coding in first-order vibrissa afferents of rats. 1. Receptive field properties and threshold distributions. Somatosens Res 1:51–67.

Gordon J (1991) Spinal mechanisms of motor coordination. In: Principles of neural science, 3rd edn (Kandel ER, Schwartz JH, Jessel TM, eds), pp. 580–595. New York: Elsevier.

Hartings JA, Simons DJ (1998) Thalamic relay of afferent responses to 1- to 12-Hz whisker stimulation in the rat. J Neurophysiol 80:1016–1019.

Hopfield JJ (1982) Neural networks and physical systems with emergent selective computational abilities. Proc Natl Acad Sci USA 79:2554–2558.

Hoppensteadt FC (1986) An introduction to the mathematics of neurons. Cambridge: Cambridge University Press.

Kleinfeld D, Berg RW, O'Connor SM (1999) Anatomical loops and their electrical dynamics in relation to whisking by rat. Somatosens Mot Res 16:69–88.

Kleinfeld D, Sachdev RNS, Merchant LM, Jarvis MR, Ebner FF (2002) Adaptive filtering of vibrissa input in motor cortex of rat. Neuron 34:1021–1034.

Lichtenstein SH, Carvell GE, Simons DJ (1990) Responses of rat trigeminal ganglion neurons to movements of vibrissae in different directions. Somatosens Mot Res 7:47–65.

Nicolelis MAL, Baccala LA, Lin RCS, Chapin JK (1995) Sensorimotor encoding by synchronous neural ensemble activity at multiple levels of the somatosensory system. Science 268:1353–1358.

O'Connor SM, Berg RW, Kleinfeld D (2002) Coherent electrical activity along vibrissa sensorimotor loops during free whisking in rat. J Neurophysiol 87:2137–2148.

Perkel DH, Bullock TH (1968) Neural coding. Neurosci Res Program Bull 6:221–248.

Perkel DH, Schulman JH, Bullock TH, Moore GP, Segundo JP (1964) Pacemaker neurons: effects of regularly spaced synaptic input. Science 145:61–63.

Rumelhart D, McClelland JL (eds) (1986) Parallel distributed processing, vols I and II. Cambridge, MA: MIT Press.

Schoner G, Kopecz K, Spengler F, Dinse HR (1992) Evoked oscillatory cortical responses are dynamically coupled to peripheral stimuli. Neuroreport 3:579–582.

Seung HS (1996) How the brain keeps the eyes still. Proc Natl Acad Sci USA 93:13339–13344.

Sherman SM, Guillery RW (1996) Functional organization of thalamocortical relays. J Neurophysiol 76:1367–1395.

Shoykhet M, Doherty D, Simons DJ (2000) Coding of deflection velocity and amplitude by whisker primary afferent neurons: implications for higher level processing. Somatosens Mot Res 17:171–180.

Silva LR, Amitai Y, Connors BW (1991) Intrinsic oscillations of neocortex generated by layer 5 pyramidal neurons. Science 251:432–435.

Sosnik R, Haidarliu S, Ahissar E (2001) Temporal frequency of whisker movement. I. Representations in brain stem and thalamus. J Neurophysiol 86:339–353.

Talbot WH, Darian-Smith I, Kornhuber HH, Mountcastle VB (1968) The sense of flutter-vibration: comparison of the human capacity with response patterns of mechanoreceptive afferents from the monkey hand. J Neurophysiol 31:301–334.

Wessberg J, Stambaugh CR, Kralik JD, Beck PD, Laubach M, Chapin JK, Kim J, Biggs SJ, Srinivasan MA, Nicolelis MA (2000) Real-time prediction of hand trajectory by ensembles of cortical neurons in primates. Nature 408:361–365.

White EL, Keller A (1987) Intrinsic circuitry involving the local axon collaterals of corticothalamic projection cells in mouse SmI cortex. J Comp Neurol 262:13–26.

Wiener N (1949) Cybernetics. New York: John Wiley.

Zucker E, Welker WI (1969) Coding of somatic sensory input by vibrissae neurons in the rat's trigeminal ganglion. Brain Res 12:138–156.